Inorganic Replication in Electron Microscopy

By C. J. CALBICK

Contrast and resolution in electron micrographs from thin replica films are determined by the geometrical relationships between the directions of incidence of the condensing atom beam and the local surface normal, during film formation by evaporation *in vacuo*, and the direction of incidence of the electron beam, during subsequent exposure in the microscope. Replica films may be formed of any material suitable for vacuum evaporation. Metal atoms in general tend to stick where they strike, moving only short distances, 100 Å or less, to nucleating centers where they form small crystallites. Oxides such as silica and silicon monoxide, and also the semi-metal germanium, form amorphous films. A portion of the incident material, about 50% in the case of silica, migrates large distances, 5000 Å or more, before finally condensing; the remainder sticks where it first strikes the surface.

The existence of a minimum perceptible mass thickness difference, about 0.7 $\mu g/cm^2$ for 50 kv electrons, results in an optimum replica mass thickness of about 10 $\mu g/cm^2$. The resolution of the replica film is proportional to its linear thickness and hence is inversely proportional to its density. Micrographs of silica, chromium, gold-manganin, aluminum, aluminum-platinum-chromium and germanium replicas are shown. The importance of stereoscopic methods in interpretation of micrographs is discussed.

THE basic purpose of micrography of surfaces is to exhibit structural topography. Present day electron microscopes are transmission-type instruments. Practical limitations of experimental technique establish a voltage of the order of 50 kv as the most useful accelerating potential for the electrons used for illumination. In bright field transmission microscopy, the image consists of a field with local variations of intensity produced because the object has partially absorbed, or scattered, the incident radiation. In electron imaging scattering is the predominant factor, limiting direct examination to objects whose mass thickness does not exceed about 50 $\mu g/cm^2$.* Thicker specimens can be examined only in profile.

Optical microscopy of surfaces is concerned with their appearance as seen by reflected light, the counterpart of which is not practicable[1] with electrons. The electron microscopist has therefore devised means of transferring surface structural details to thin films called replicas.[2] These films must present to the electron beam locally varying thickness corresponding to the surface details. A simple type is the plastic replica[3] consisting of an appropriately thin plastic film stripped from the surface. A second type

* Some microscopes provide a range of accelerating potentials, up to 100 kv or more, permitting direct examination of thicker objects.

[1] Zworykin et al. "Electron Optics and the Electron Microscope," pp. 98–106.

[2] *J. Roy. Micro. Soc., 70*, 1950, "The Practise of Electron Microscopy," ed. by D. G. Drummond, see Chapters II and V.

[3] V. J. Schaefer and D. Harker, *Jl. App. Phys., 13*, 427 (1942).

is the oxide film,[2] produced by controlled oxidation of the surface when it is aluminum or another suitable metal. For other materials, a pressure mold of the surface in pure aluminum may be utilized as an intermediate replica in a two-step process.[4] A third type is the silica replica,[5] [6] produced by the condensation of silica vaporized by a hot source *in vacuo*, either on the surface in a one-step, or on a plastic mold of the surface in a two-step, process. A fourth type is the shadow-cast plastic replica,[7, 8] produced by similar deposition of a suitable metal at near-glancing incidence upon a plastic replica.

The purpose of this paper is to discuss the process of evaporated film formation as it is related to properties important in microscopy. The resolution and range of contrast available in the finished micrograph determine the faithfulness with which the original surface is depicted, and depend on the relative orientation of the surface, vapor source, and electron beam, on the density and average thickness of the replica, and on the mechanism of condensation. In principle, it is pointed out that any material of suitable physical and chemical properties may be used for evaporated replica films, and a number of examples are shown in micrographs. Inorganic replica films retain the third or vertical dimension, a fundamental advantage which permits stereoscopic study. The material presented perhaps provides a unified view of replication techniques and a method for the evaluation of micrographs relative to the faithfulness of portrayal of the original surface.

1. Local Thickness of Condensed Material

Figure 1 illustrates how the thickness t_e in the direction of the electron beam is dependent on the local surface normal n. The thickness t_a in the direction of the atom source is constant, depending only on the amount of material reaching the surface. The thicknesses due to two or more sources obviously may be vectorially added, and hence *an arbitrary assembly of sources may be replaced by a single source properly located*, since each yields the same thickness distribution on the surface S. A simple analogy is the shading produced when ordinary objects are illuminated by direct light. It is clear that atom source and electron beam must differ in direction for shading to occur. The atoms or molecules of some materials, notably silica and silicon monoxide, do not all stick where they strike, but some wander over the surface[9] as a "two-dimensional gas" before condensing. This

[4] J. Hunger and R. Seeliger, *Metallforschung*, *2*, 65 (1947).
[5] R. D. Heidenreich and V. G. Peck, *Jl. App. Phys.*, *13*, 427 (1943).
[6] C. H. Gerould, *Jl. App. Phys.*, *17*, 23 (1947).
[7] H. Mahl, *Korrosion u. Metallschutz*, *20*, 225 (1945).
[8] R. C. Williams and R. W. G. Wyckoff, *Jl. App. Phys.*, *17*, 23 (1946).
[9] R. D. Heidenreich, *Jl. App. Phys.*, *14*, 312 (1943).

results in a somewhat different shading distribution. The distributions are mathematically formulated in Appendix I.

1.1 *Shadows*

In certain regions the local surface is not exposed to the source, resulting in "shadows" within which t_e is zero. These shadows are bounded by two lines, the shadow-casting profile and the shadow edge. The shape of the shadow edge depends both on the shadow profile and on the topography in the vicinity of the edge and in consequence interpretation of shadowing is

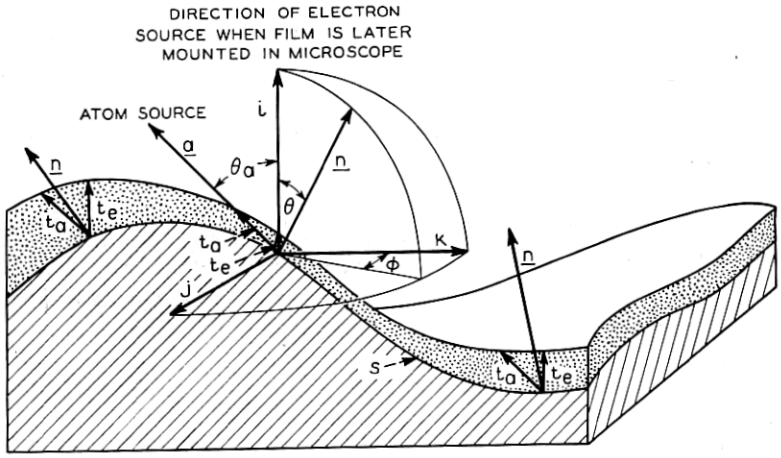

Fig. 1—Diagrammatic representation of thin film replicas produced when every atom sticks where it strikes.

difficult unless one of the surfaces is smooth.[10] With multiple or extended sources, partial shadows and shading due to partial shadowing occur.

1.12 *Negative shadows*

There may be other regions of the surface which are exposed to the atom source, but not to the subsequently incident electron beam. When the replica film is mounted in the microscope, these regions appear reentrant to the electron beam, which must pass through three rather than one layer of replica. These regions appear as very lightly exposed areas in micrographs, and since they are essentially "negative shadows" are subject to the same considerations of shape and interpretation as ordinary shadows.

[10] "Physical Methods in Chemical Analysis," Vol. 1, 1950. On pp. 571–3, R. D. Heidenreich reports some unpublished work of S. G. Ellis and W. G. Gross, showing great differences in appearance of shadow-cast replicas as the azimuth of the atom source is varied.

2. Intrinsic Resolution of Replica Films

In the vicinity of a sharp change in surface gradient, the local thickness t_e does not change abruptly, but the change occurs over a short distance d as illustrated in Fig. 2. A mathematical formulation for this intrinsic resolution d is given in Appendix II, with some detailed discussion. Intrinsic resolution varies locally over the surface, dependent on the geometrical relationship between atom source, electron beam, and local surface topography. *Observable* resolution includes also instrumental resolution and contrast factors. Except at shadow boundaries it is probably never less than $\frac{1}{2}\bar{t}_e$, where $\bar{t}_e$ is the average value of t_e, and perhaps may be as poor as

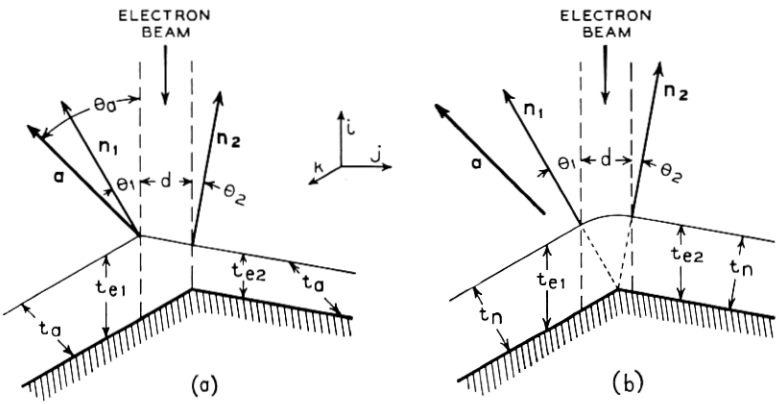

Fig. 2—Diagram showing resolution of replica film at a sharp corner. (a) Every atom sticks where it strikes. (b) All atoms diffuse, finally condensing into film of uniform local thickness.

several times $\frac{1}{2}\bar{t}_e$. Shadow profiles and edges often show short lengths of extreme sharpness. The resolution across these portions of shadows may often be assumed to be the instrumental resolution. The reasons for this are developed in the Appendix.

2.1 *Effect of Film Thickness*

The average linear thickness $\bar{t}_e$ is a factor in the expressions for resolution. To reduce d and thereby improve the resolution, the most effective method is to reduce $\bar{t}_e$. With a given material, as the replica film is made thinner, the contrast is reduced also, so that, just as in photography a feature that is visible in a properly exposed negative may be lost in a thin negative, some features may not be replicated with sufficient contrast to be detectable. For 50 kv electrons, the *optimum* average thickness of a replica lies between 5 and 10 $\mu g/cm^2$. This is 7–15 times the minimum perceptible thickness

difference, a rule applicable for electrons of any energy. The local thickness of the replica varies from a fraction of to several times its average thickness, and a replica of near optimum thickness provides a range of 20–40 detectably different shades of contrast. Although for special purposes a replica film may be made thinner or thicker, usually the average thickness should be selected in the optimum range. The resolution is then determined by its density, or more precisely, by its electron scattering power. Because the denser materials are composed of elements of higher atomic number which are more efficient scatters, scattering power† tends to increase rather faster than density, but the difference is not sufficiently great to invalidate for

TABLE I
RESOLUTIONS OF REPLICA FILMS
10 $\mu g/cm^2$

Film Material	Density	$\bar{l}_e$	Resolution $\frac{1}{2}\bar{l}_e$
Plastic	1	1000 Å	500 Å*
Silicon	2.4	416	208
Silica (Silicon Monoxide)	2.5	400	200
Aluminum	2.7	370	165
Aluminum oxide	3.7	270	135
Germanium	5.4	185	92
Chromium	6.9	144	72
Gold 50%**, Manganin 50%	14	72	36
Gold 67%**, Manganin 33%	16	62	31
Uranium	18.7	50	25***
Gold	19.3	50	25
Platinum	21.5	44	22

* Included for comparison only.
** By volume.
*** On exposure to air, *U* oxidizes.

the present purposes the assumption that the two are proportional. The existence of an optimum average mass thickness then implies that *intrinsic resolution of replica films is inversely proportional to the density of the material of which they are composed.*

Table I presents a comparison of the resolutions associated with various materials, based on the assumption that the resolution is $\frac{1}{2}\bar{l}_e$. As discussed above, this is about the best observable resolution, for favorable topographic features. The resolution of plastic films is not susceptible to calculation, and is probably greater than indicated. The resolutions of evaporated films decrease from about 200 Å for silicon and silica to about 25 Å for the very heavy metals. However, it is difficult to process the exceedingly thin films of these metals particularly if they recrystallize as does gold. Although

† Ref. 1, Chap. 19 and p. 158. See also C. E. Hall, *Jl. App. Phys. 22*, 658, 1951.

gold-manganin films are only slightly thicker, they are not particularly difficult to process, especially if 500-mesh supporting screen is used.

2.2 *Granularity*

Resolution is also affected by the short-range migration which culminates in recrystallization of many metallic films.[11, 12, 13, 14] If the crystallite size is smaller than the resolution, i.e. less than $\frac{1}{2}l_e$, this effect is not too important, even though the granularity may be objectionable at high magnification from an esthetic viewpoint. A fairly extreme example of recrystallization is shown by the aluminum replica in Fig. 9.

A second source of granularity is due to properties of plastics when plastic molds are used as intermediate replicas. Because plastic molecules are large, and because they associate into domains,[15] the plastic surface is actually granular on a scale of the order of 100 Å. Plastic granularity is not observed in silica replicas because of insufficient resolution, but it becomes very evident in shadow-cast replicas on account of the near-glancing incidence of the shadowing material.[16, 17] The occurrence of granularity due to this cause in replica films of denser materials is an indication of their good resolution. Since this granularity is real on the plastic surface, it shows clearly the azimuth of the incident atom beam, whereas granularity due to recrystallization shows no directional effect.

3. Experimental Observations

The foregoing material presents a rather idealized picture of the process of replica film formation by condensation of inorganic substances evaporated under good vacuum, i.e. at pressures preferably less than 10^{-5} mm, and certainly not greater than 10^{-4} mm of mercury. Subsequent to film formation in the vacuum, it must be subjected to gross physical and chemical processing to prepare it for electron microscopic examination. It must be exposed to air, which may cause oxidation. Uranium films, for example, appear to oxidize completely, and it is believed that SiO films oxidize to SiO_2. Most metal films yield good electron diffraction patterns characteristic of the metal, although this does not preclude the possibility of surface oxidation, since the oxides are usually amorphous and diffuse rings due to thin oxide layers would be difficult to detect. Then the films must be sepa-

[11] R. G. Picard and O. S. Duffendack, *Jl. Appl. Phys.*, *14*, 291 (1943).
[12] H. A. Stahl. *Jl. Appl. Phys.*, *20*, 1, (1949).
[13] H. Levinstein, *Jl. Appl. Phys.*, *20*, 306 (1949).
[14] R. S. Sennett and G. D. Scott, *Jl. Opt. Soc. Am.*, *40*, 203 (1950).
[15] C. C. Hsiao and J. A. Sauer, *Jl. Appl. Phys.*, *21*, 1070 (1950).
[16] R. C. Williams and R. C. Backus, *Jl. Appl. Phys.*, *20*, 98 (1949).
[17] Metallurgical Applications of the Electron Microscope, p. 11, *Symp. of Inst. of Met.*, November 1949.

rated from the surface replicated, usually by dissolution of the latter. This process subjects the film to considerable strain. Finally it must be removed from the solvent, usually on a piece of 200-mesh screen, rinsed at least once, and finally allowed to dry. It is not surprising that films sometimes

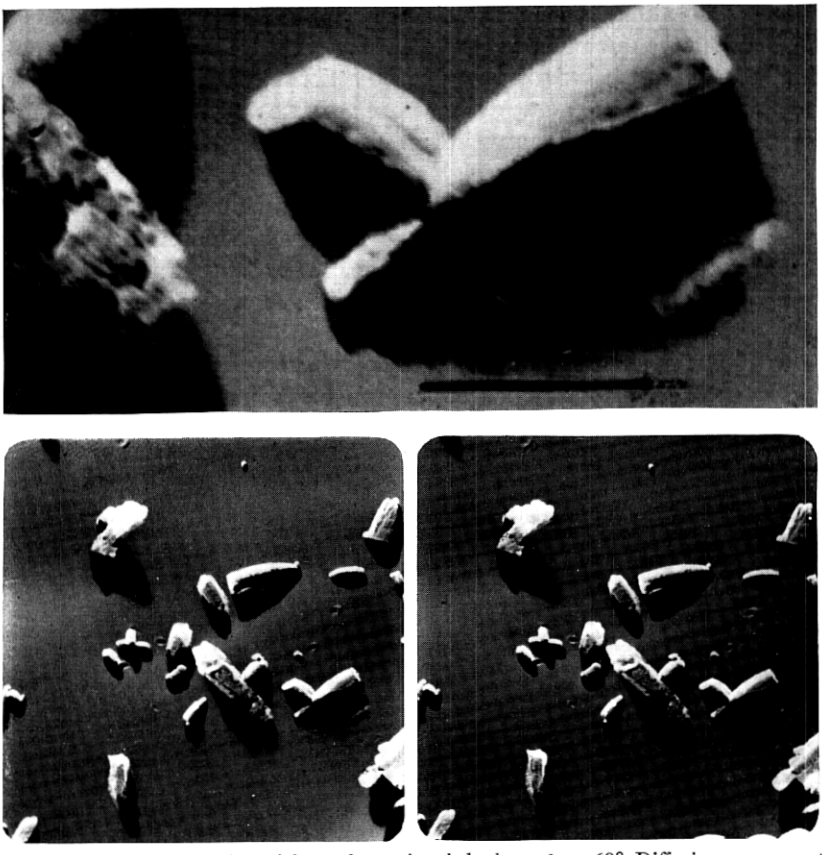

Fig. 3—Silica replica of particles and associated shadows. $\theta_a = 60°$. Diffusing component replicates particles within shadows. Oval hole shows presence of film in shadow. Black lines = 1 μ.

exhibit cracks and holes. Stereoscopic examination of good replicas show that despite all the processing violence, a faithful picture of surface topography is obtained, at least for features up to a few microns in size.

The nature of silica condensation is indicated by the micrographs of Fig. 3, of a silica replica of particles of an alkaline earth carbonate. These were dispersed on a plastic-coated microscope slide, and silica evaporated at

$\theta_a = 60°$. The plastic film was then "floated off" on water and picked up on 200-mesh screen; the plastic and particles were successively dissolved, leaving the silica replica.† The micrographs clearly show (a) shadow-edges and (b) a film in the shadows. The enlargement shows a shadow within which there exists a hole in the film and replication of completely shadowed particles by the diffusing component. It follows from (a) that a part of the incident material must stick where it strikes, and from (b) that a part must diffuse into the shadows, somewhat in the manner diagrammatically illustrated in Fig. 4. Densitometer traces through shadow edges show that the film thins down a little as the edge is approached from the unshadowed region, drops more or less abruptly at the edge, and continues to thin down within the shadow as illustrated. Now the diffusing part must finally con-

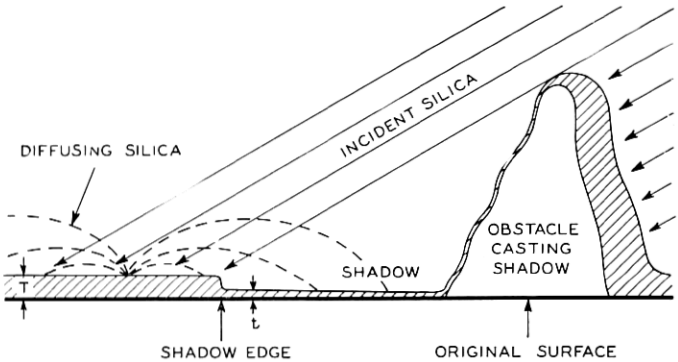

Fig. 4—Diagram illustrating diffusion of silica into shadowed regions.

dense, and it is natural to assume that at each collision with the surface the probability of sticking is α, and of diffusing is $(1 - \alpha)$, and that the average molecule travels between collisions a small distance. Analysis of densitometer curves on these assumptions leads to a value of α of about $\frac{1}{2}$, and a range of about $\frac{1}{2}\ \mu$, with a rather wide spread of values.[18] However, these assumptions would require the film to be vanishingly thin at distances more than $3\ \mu$ from the shadow-edge. In fact, an *extremely* thin film is found at even greater distances. The probability of sticking upon collision, and the distance a molecule moves as a two-dimensional gas molecule between collisions with the surface, thus must be assumed to depend on such factors as angle of impingement, energy of molecule, and perhaps the nature of the surface. This latter initially is a plastic, probably covered

† In particle study, a second evaporation of silica 180° in azimuth from the first produces a "thin-shell" replica more suitable for stereoscopic study of the particles.

[18] C. J. Calbick, *Jl. Appl. Phys.*, *19*, 119 (1948).

with adsorbed gas, and later during the deposition is freshly condensed silica. Films are also found in shadows of replicas made of other materials such as silicon monoxide, germanium, gold-manganin, and even chromium. Whether the interpretation should always be the same as for silica, or whether in some cases the diffusing component is different from the sticking component, is uncertain.

A high degree of contrast is commonly attributed to silica replicas, which are supposedly deposited at near-normal incidence. In the writer's experience, distortion of the conical-tungsten-basket silica evaporator often results in values of θ_a greater than 10°. If normal incidence, characterized by absence of shadows, is actually attained, the resulting replica exhibits

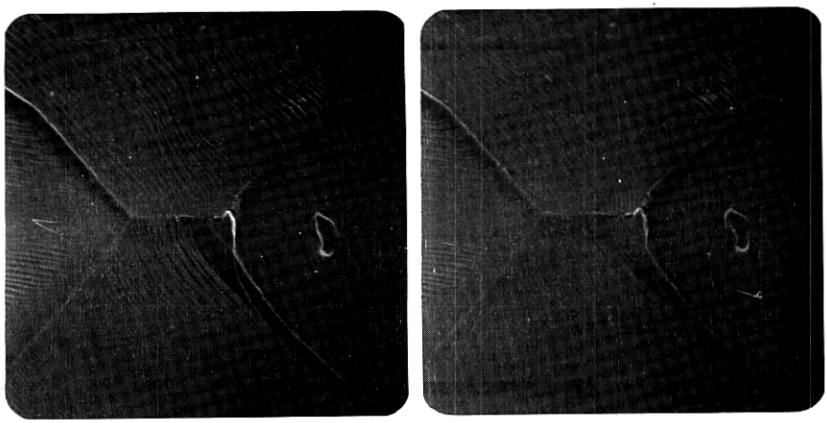

Fig. 5—Silica replica of natural surface of thermistor flake heated to 1425°C. Note difference in contrast between the two pictures of the stereogram.

poor contrast unless steep slopes are present. An example is shown in Fig. 5, in which difference in contrast due to the fact that θ_a differs for the two pictures of the pair by approximately 8°, the stereoscopic angle, is evident. Note that the shadow in the surface feature in the center of the grain at the right is more pronounced in the left-hand picture which shows the greater contrast. The replica is from the surface of a thermistor flake, sintered briefly at 1425°C.

Figure 6 is from a silica replica about 400 Å thick, of a portion of the surface of a thermistor disk sintered 6 hrs. at 1175°C. The white line is 0.1 μ long. The striations show a minimum separation of about 250 Å, and the character of the shading indicates that this is near the limit of resolution of the micrograph, about 200 Å (Table I). Higher resolutions claimed[5, 9] are probably due either to shadow effects, to special situations on the sides of steep slopes, or perhaps to the use of extremely thin replicas.

The natural surfaces of sintered thermistor flakes, prepared by heating in air thin (10 μ) sheets of a mixture of NiO and Mn_2O_3 powders, exhibit well defined planes of sizes suitable for electron micrographic study.[19] Flakes sintered briefly at 1175°C were selected as suitable objects for experimental study of replication. They were molded into the surface of lucite blocks at 150–160°C and 2500 lb/in^2. They were then dissolved in HCl,§ and replica

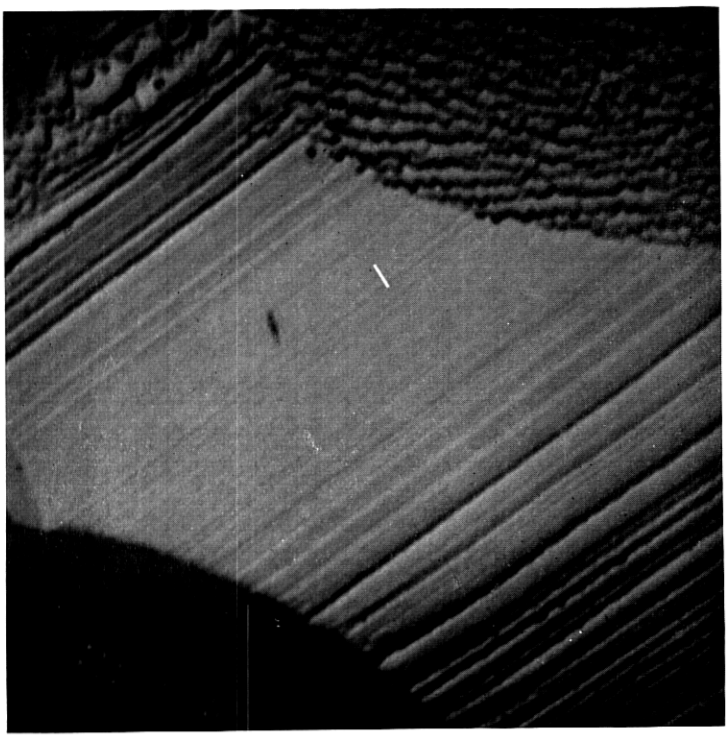

FIG. 6—A striated region on the surface of a thermistor disk. White line = 0.1 μ. Striations are near the limit of resolution of the silica replica, which is about 400Å thick.

films deposited on the plastic molds at pressures not greater than 10^{-4} mm (usually about 2×10^{-5} mm). The replica surface was then scored into small (about 1.5 mm) squares and immersed in ethyl bromide.¶ In a few minutes the replica films drift free and are then "fished" from the solvent

[19] H. Christensen and C. J. Calbick, *Phys.Rev.*, *74*, 1219 (1948).

§ A one-step process was precluded because some of the replicating materials are soluble in HCl.

¶ Ethyl bromide is not a good solvent for lucite, while chloroform is. Extended tests have produced better results when a poor solvent, which perhaps frees the replica by creeping between it and the plastic mold without appreciable dissolution, is used.

on pieces of 200- or 500-mesh screen. After drying, the screen is immersed in chloroform to remove the last traces of plastic, and is then ready for electron microscope use.

The electron micrographs of Figs. 7–11 are presented as stereoscopic pairs and enlargements of selected areas, the scale being given by dark lines of 1 μ length. Figure 7 is a micrograph from a chromium replica[20] for which

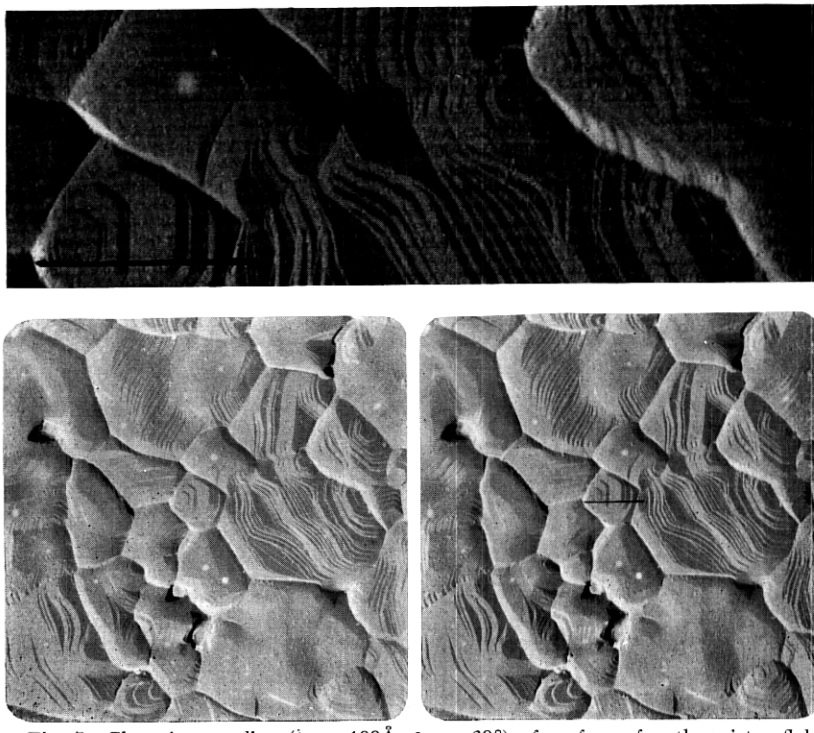

Fig. 7—Chromium replica (t_e = 100Å, θ_a = 30°) of surface of a thermistor flake. Resolution about 50Å. Granularity is due to plastic mold.

t_e = 100 Å, θ_a = 30°. The shadows show that the azimuth of incidence was to the right at about 30° above the horizontal. The granularity evident in the enlargement shows evidence of this direction, and may be ascribed to plastic granularity, except for a few of the larger hills or pits which are

[20] J. Ames, T. L. Cottrell and A. M. D. Sampson, *Trans. Far. Soc. 46*, 938 (1950). This paper, which appeared while the present paper was in preparation, exhibits micrographs of chromium and other metallic replicas of surfaces of crystals grown from solution. The characteristic surface structures reported are in some ways similar to those of the sintered thermistor flakes here shown.

probably due to features of the original surface. Resolution ranges upward from about 50 Å.

The detection of films in shadows is difficult when these films are so thin as to approach the minimum perceptible thickness difference. The film may be flawless and present, or ruptured during processing and completely eliminated, and the difference between these two conditions is difficult to

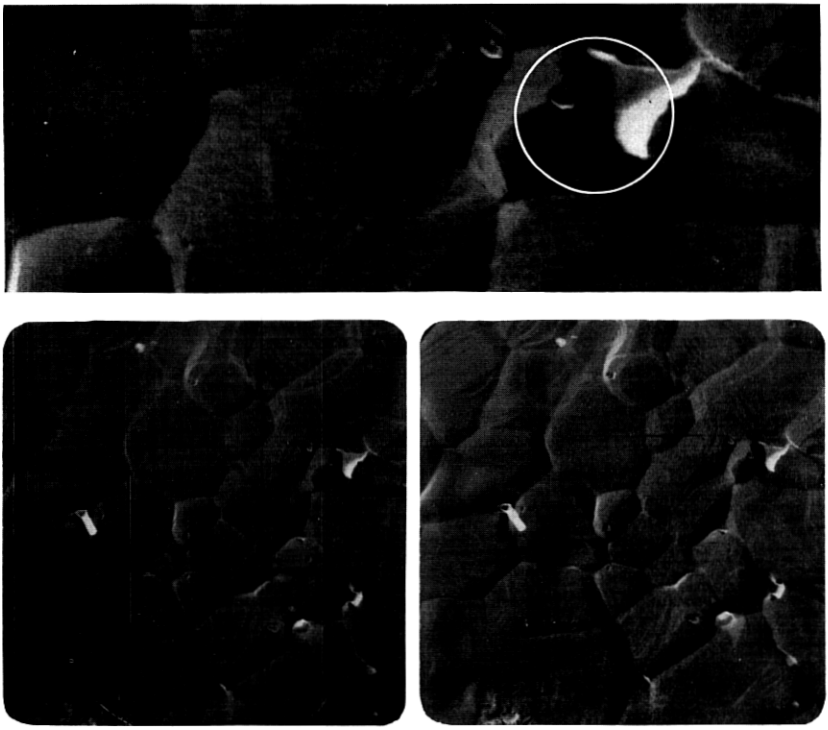

Fig. 8—Chromium replica (t_e = 150Å, θ_a = 30°) produced by two evaporations differing in azimuth by 90°. Region within the circle shows partial shadows.

discern. Only when structure or edges due to partial rupture appear is it easily detectable. Some shadows in the replica from which Fig. 7 was made showed such a film, which was estimated to be less than 10 Å in thickness, but in most of the shadows no evidence of a film could be seen.

A chromium replica produced by two evaporations, from azimuths 90° apart, was the subject of the micrograph of Fig. 8. This replica was not washed in chloroform, which accounts for the presence of the residual plastic rings. This particular micrograph was selected to show the partial

shadowing effect shown clearly in the enlargement, but is not suitable for determination of resolution or exhibition of plastic granularity on account of the slightly imperfect focus, noticeable in the enlargement. Because the replica was about 150 Å thick, this granularity was scarcely evident even in a perfectly focused micrograph, from which the resolution was estimated as ranging upward from about 100 Å. It should be observed that the direction

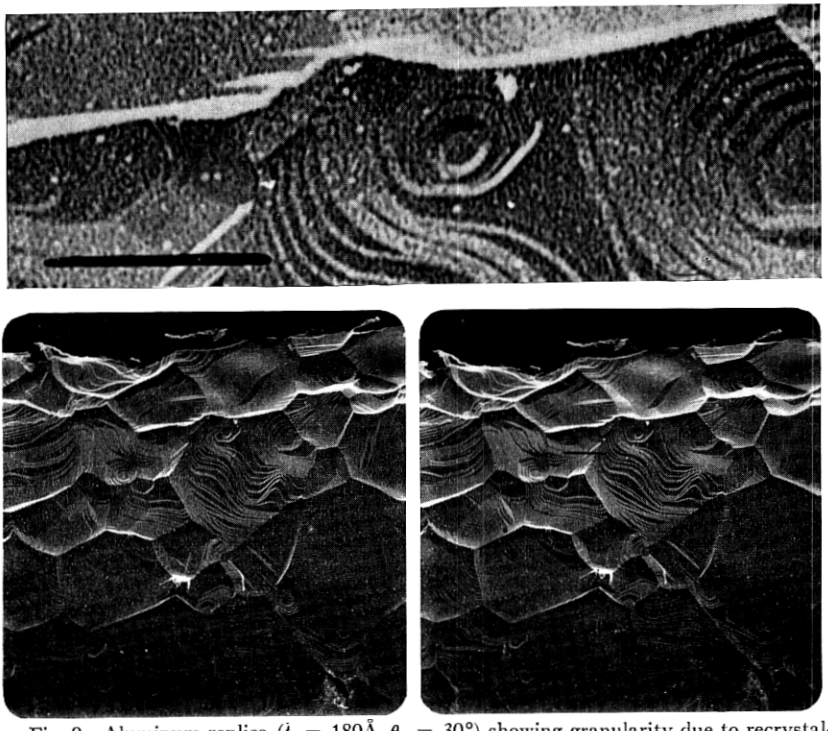

Fig. 9—Aluminum replica (l_e = 180Å, θ_a = 30°) showing granularity due to recrystallization. Local curling of replica has resulted in "negative shadows" in upper left region of stereogram. Resolution about 100Å.

of maximum contrast in shading is as if a single source were toward the lower right, about midway between the two actual sources whose azimuths can be determined in the stereogram.

The appearance of a micrograph of a replica which has undergone recrystallization on a scale comparable to l_e is shown in Fig. 9. The replica was of aluminum; l_e was about 180 Å, the lower limit of the optimum range; θ_a was 30°. The non-directional character of the granularity is evident. The micrograph selected shows an area near a torn edge which has curled up-

ward, thus tilting the replica to various angles. In the extreme upper left, this tilt produces *negative* shadows, regions where the electrons pass through three thicknesses of replica. In none of the more usual positive shadows observed in other parts of the replica was any film observed, or in a replica twice as thick also studied. The conclusion is that aluminum does not diffuse. It is tempting to speculate that the short-range forces responsible

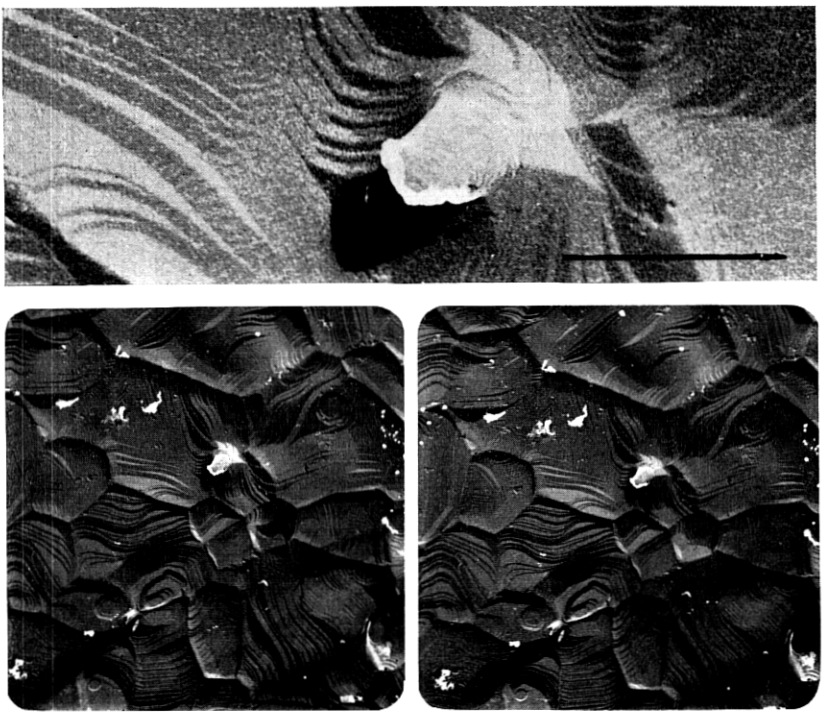

Fig. 10—Gold-manganin replica (t_e = 150Å, θ_a = 20°). Resolution about 100Å. Replica is much thicker than optimum. A film in the shadow, clearly evident in the original micrograph, does not show except for two whitish areas where it has torn and curled.

for recrystallization do not permit diffusion and, that when diffusion does occur with materials such as chromium, it is due to some other component such as an oxide. Resolution, although complicated by the granular structure, appears to be about 100 Å.

The micrograph of Fig. 10 is from a gold-manganin replica, produced by simultaneous evaporation of two volumes of gold and one of manganin (alloy, 84% Cu, 12% Mn, 4% Ni) at θ_a = 20°. The total thickness was about 150 Å, so mass thickness, about 24 $\mu g/cm^2$, was much greater than the

optimum. Crystallite size is probably less than 50 Å. As in Fig. 10, the granularity is probably due to plastic. A thin, torn film appears in the shadow. From the extreme sharpness of a portion of one edge of the shadow, although slightly complicated by granularity, one concludes that instrumental resolution is better than 50 Å. Replica resolution is about 100 Å. Despite the smaller value of θ_a, the thick replica provides a greater range of tone

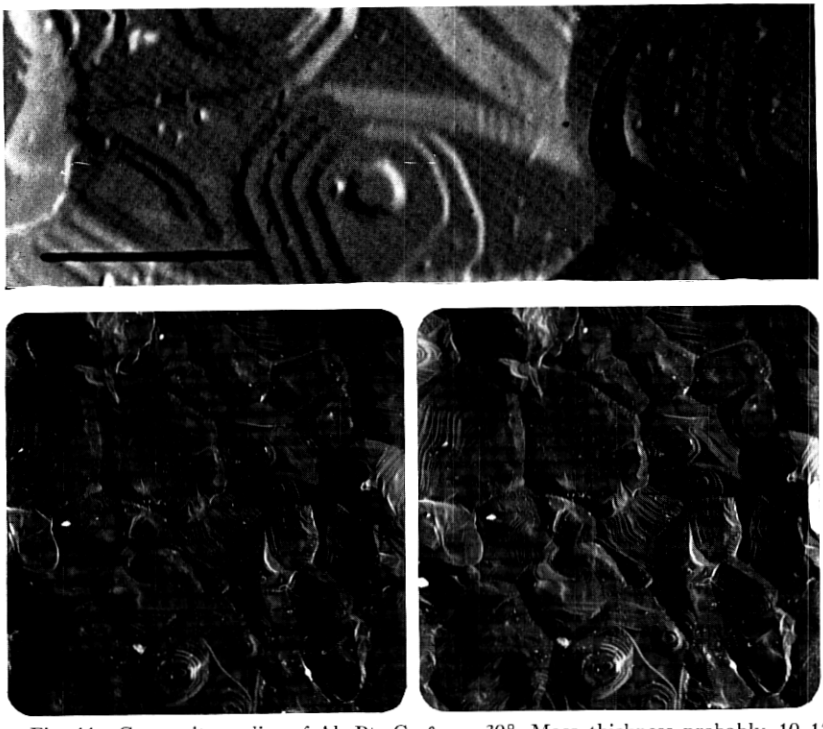

Fig. 11—Composite replica of Al, Pt, Cr. $\theta_a = 30°$. Mass thickness probably 10–12 $\mu g/cm^2$. Resolution about 100Å.

values, as compared with Fig. 7, although this may not be evident in the reproductions.

Figure 11 shows a micrograph from a composite replica of aluminum, platinum, and chromium. Aluminum and platinum were simultaneously evaporated from a tungsten wire which burned out before the evaporation was complete. If all the aluminum evaporated before the platinum, its thickness was about 50 Å. The amount of Pt is problematical, but the chromium, evaporated after the tungsten wire was replaced, had a thickness of about 100 Å. The same angle, $\theta_a = 30°$, was used in the two evaporations.

The granularity barely discernible in the enlargement, which again shows a slight imperfection in focusing, is attributable to plastic. Resolution is perhaps 100 Å.

Metallic film replicas could easily be used to replicate surfaces in sealed-off tubes. For example, chromium can be plated on a tungsten wire which is suitably mounted in the tube, and thoroughly outgassed during pumping, the surface to be replicated being shielded from the Cr source during the process. Later it is evaporated to form the replica. As an illustration, Fig. 12 is from a Cr replica of the activated surface of an oxide-coated cathode. It was actually prepared by evaporation at a pressure of 2×10^{-6} mm and not in a sealed-off tube, but the suggested technique is certainly practicable. No films were observed in shadows in this replica, which was less than

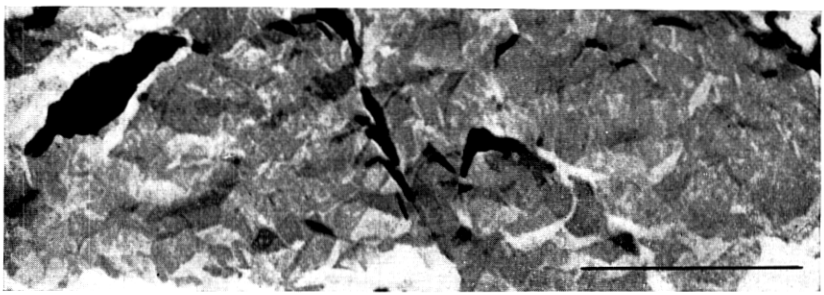

Fig. 12—Chromium replica (t_e = 100Å, θ_a = 30°) of surface of an oxide-coated cathode. One-step replica. Whitish areas are due to impurity in the oxide (probably silica) redeposited on the replica.

100 Å thick with $\theta_a = 30°$. However, the film was very flimsy and exhibited a large number of cracks, usually originating in shadows (e.g., the elongated black area). The film was freed from the surface by dissolving the oxide in dilute acid; since no plastic mold was involved, the fine scale features are characteristic of the oxide surface. The whitish areas (near bottom) are due to some impurity in the oxide redeposited on the replica, probably silica from the ball-milling process to which the original barium carbonate powder had been subjected. Replica resolution is perhaps 100 Å, although suitable features to test higher resolving power are not present. Shadow edges indicate instrumental resolution less than 50 Å.

In Figs. 13 and 14 the use of germanium as a replicating material is illustrated. Germanium is easily evaporated from a conical carbon crucible supported and heated by a conical helix of tungsten. As in the case of silica and silicon monoxide, the thickness of the resulting film is only roughly known. For the replica of Fig. 13, 2 mg of Ge at 8 cm distance, $\theta_a = 30°$,

was used, and $\bar{l}_e$ is estimated to lie between 200 and 300 Å. For that of Fig. 14, 1 mg at 8 cm with $\theta_a = 35°$ was used and $\bar{l}_e$, between 100 and 150 Å, is in the optimum thickness range. The micrograph has the appearance of a correctly exposed photographic negative, whereas Fig. 13 resembles an over-exposed negative. Since germanium films are amorphous unless heated to temperatures higher than 300°C, the fine structure is perhaps due to

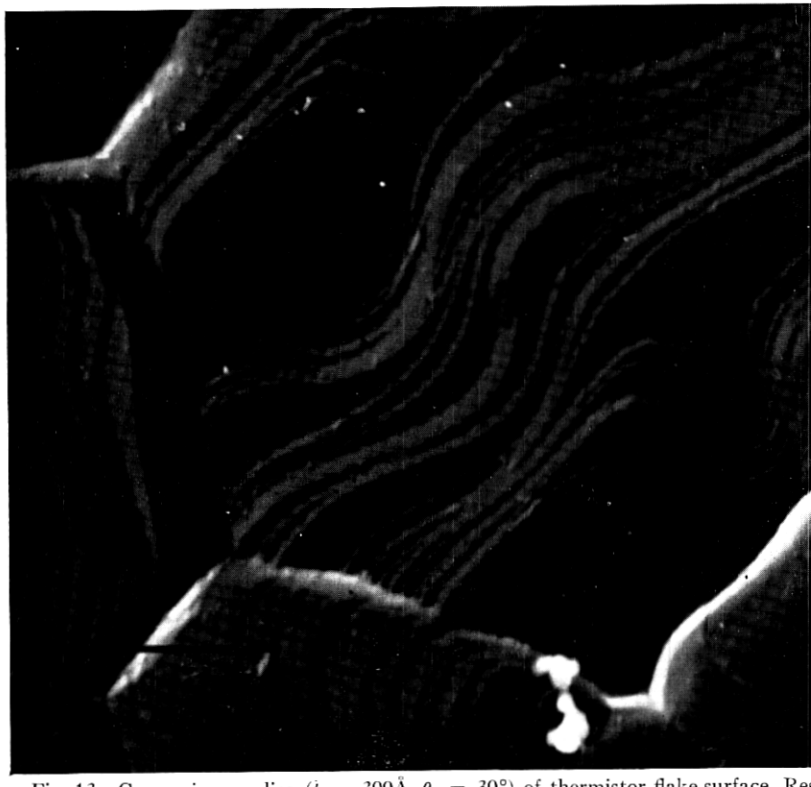

Fig. 13—Germanium replica ($\bar{l}_e \simeq 300$Å, $\theta_a = 30°$) of thermistor flake surface. Resolution about 150Å. Over-exposed appearance shows replica is thicker than optimum.

plastic granularity, although some features are probably real in the thermistor flake surface. Resolutions are perhaps 150 Å (Fig. 13) and 75 Å (Fig. 14). A film clearly appears in the shadow in Fig. 14. Germanium shadow films are relatively thinner than silica, indicating that α is greater than 0.5 (perhaps 0.7 to 0.8), but thicker than chromium or gold-manganin shadow films.

Germanium has many advantages as a replicating material. It is easily

evaporated; the films are substantially amorphous; they are fully as rugged as silica films in processing and, in contrast to silica films, are easily seen during the "fishing" part of this procedure. Because they are conducting and do not tend to charge up in the microscope, germanium films are more stable than silica. Finally, and most important, because germanium is

Fig. 14—Germanium replica ($t_r \simeq 150$Å, $\theta_a = 35°$) of near optimum thickness. Resolution about 75Å. Ruptured film evident in shadow.

twice as dense as silica, the intrinsic resolution (Table I) is better by a factor of two. Many of these remarks apply also to chromium and gold-manganin replicas; however, they are not amorphous and are less rugged in processing, even though they are perhaps even more stable in the microscope. Stereoscopic pairs from germanium replicas are not shown only because it is desired to present the more extensive enlargements of Figs. 13 and 14.

Figure 15 shows electron diffraction patterns obtained from the several replica films, indicating that crystallite size ranges from greater than 100 Å for aluminum down to almost amorphous for germanium and amorphous for silica.

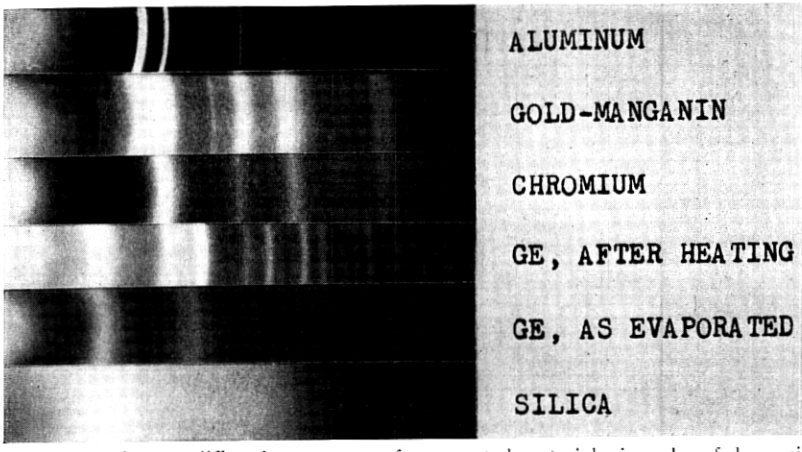

Fig. 15—Electron diffraction patterns of evaporated materials, in order of decreasing crystallite size. The aluminum pattern is due to crystallites of about 100Å. The gold-manganin pattern shows at least two sharp rings not due to gold and diffuse bands due to very small crystallites with the structure of gold. The chromium pattern is due to very small crystallites of Cr. The pattern of a germanium replica film after heating in air to 390° shows partial recrystallization, with rings due to quite small crystallites superposed on the amorphous pattern of the Ge as evaporated.

4. Interpretation of Micrographs of Replicas

The electron image pattern due to the replica is reproduced by the exposure of a photographic plate. The complex problems associated with photographic reproduction[21] cannot be discussed here. For a number of reasons, blackening of the plate is not linearly related to replica film thickness. The number of electrons scattered out of the beam* is proportional to thickness only as a first approximation, the blackening vs. exposure curve of the plate is not linear, and there is also a roughly uniform background due to inelastically scattered electrons. At the lower electronic magnifications, field distortion is also a factor affecting local intensity in the electron image. Furthermore, the geometrical relation between the electron beam incident upon the thin mesh-supported film and the atom-beam is usually not known accurately, and indeed may vary locally over the replica in the manner of which Fig. 9 is an extreme example. In con-

[21] W. T. Wintringham, *Proc. I. R. E.*, *38*, 1284 (1950).
* Ref. 1, ch. 19 or ref. 7, p. 541.

sequence of these factors, *the precise interpretation of density variations in micrographs is not practicable.* Also many replicas contain artifacts, i.e., features in the micrograph not due to the original surface, but introduced somewhere in the processing. Recrystallization, plastic granularity, specks of dirt or other foreign material, tears in the replica films, and defects in the photographic emulsion are examples of artifacts. Few micrographs are completely free of these effects.

The interpretation of micrographs therefore has as its object not so much a detailed topographical map of the surface, but rather its characteristic features, repeated in many micrographs. For example, the micrographs presented show that sintered NiO-Mn_2O_3 flakes develop grains with extensive crystallographic planar surfaces but that thick disks develop a striated or hill-and-valley surface structure on individual crystallites. In both cases the structure is very compact, pores between grains being almost nonexistent. (Incidentally, these materials can be subjected to a heating cycle in which pores are a predominant feature.) Naturally, the greater the range of contrast and the better the resolution, the more surely can characteristic features on an exceedingly fine scale be detected. In general, the method of replication which portrays best the characteristic features under study should be selected. Even in the study of a single material, more than one method may be desirable. For example, a porous structure is probably most easily reproduced by a silica replica using the two-step process, on account of the fact that the diffusing component forms films over reentrant regions not exposed directly to the source; but fine surface detail might best be revealed by a germanium or chromium replica using the one-step process.

5. Stereoscopy

Electron microscopy has a fundamental advantage in that, because of great depth of focus, stereoscopic study of surfaces at high magnification is possible. This advantage is sometimes indispensable; for example, porous structures result in complex micrograms which can be understood only by stereograms. More generally, *stereographic portrayal, by fully delineating surface topography, achieves the chief purpose of microscopy and makes unnecessary the precise interpretation of density variations.* However, resolution and contrast are important factors in stereograms.[22] It is obvious that *the replica must retain the third dimension; inorganic replicas in general do,* but thin film plastic replicas, unless heavily shadow-cast to make them effectively inorganic, change under the electron bombardment and draw down to a planar film of variable thickness.[23]

[22] A. W. Judge, "Stereoscopic Photography," p. 28.
[23] C. J. Calbick, *Jl. App. Phys., 19,* 1186 (1948).

Many artifacts are also detectable by stereoscopy. Since two pictures of the same field are available, photographic emulsion flaws are readily detected. The three-dimensional view also helps to identify many other artifacts, such as foreign material present on the replica or local wrinkling of the replica film.

Unfortunately, half-tone reproductions are not suitable for stereograms, because half-tone detail is objectionably enlarged by the viewing stereoscope. Despite this, some idea of the value of stereograms may be obtained from the figures.

Conclusions

A unified picture of replication by evaporated films has been presented. Thin-film replicas may be made by any material which can be evaporated *in vacuo* and whose physical and chemical properties are suitable. For good contrast, a considerable angle should separate the directions of incidence of atom- and electron-beams. The intrinsic resolution of the replica is about half the film thickness and is therefore inversely proportional to the density of the replicating material. Multiple point sources and sources of extended area are equivalent from a shading standpoint to a single point source properly placed. The oxides SiO and SiO_2, and presumably many others, form amorphous films, whereas the metals tend to recrystallize although the crystallite size may be less than 50 Å for some metals. Germanium, a semi-metal, forms an amorphous film. Although not dense compared to the heavy metals, it is more than twice as dense as SiO_2, and should be valuable as a replicating material because it combines electrical conductivity and high resolving power in an amorphous film and is chemically rather inert. Among the metals, chromium appears to be the most generally useful replicating material. Gold-manganin has sufficiently small crystallite size for many purposes, and is very easy to evaporate. The platinum group suffers from the disadvantage of being very difficult to evaporate.

Finally, all inorganic replica films studied retain the third dimension. Electron stereo-micrograms may be used to reveal three-dimensional topography, largely eliminating the need for correlation of photographic density variations with the surface structure.

APPENDIX I
CONTRAST IN REPLICA FILMS

(a) Local Thickness When Every Atom Sticks Where It Strikes.

Referring to Fig. 1, it is evident that:

$$t_c = t_a \frac{\underline{a} \cdot \underline{n}}{\underline{i} \cdot \underline{n}} = t_a \cos \theta_a \, (1 + \tan \theta_a \cos \varphi_a \tan \theta \cos \varphi). \qquad (1)$$

When the principal azimuth is defined by the plane containing $\underline{a}$ and i, $\cos \varphi_a = \pm 1$, and, as illustrated, $\cos \varphi_a = -1$. With more than one source, in directions $\underline{a}_1, \underline{a}_2 \cdots \underline{a}_m$:

$$t_e = \frac{(t_{a_1} \underline{a}_1 + t_{a_2} \underline{a}_2 + \cdots t_{am} \underline{a}_m) \cdot \underline{n}}{i \cdot \underline{n}} \tag{2}$$

and the mass thickness is given by

$$\rho_a t_e = \left(\sum_{j=1}^{m} \frac{\rho_j t_{aj} \underline{a}_j \cdot \underline{n}}{i \cdot \underline{n}} \right) \tag{3}$$

where ρ_j is the density of the material deposited by the source $t_{a_j} \underline{a}_j$, and ρ_a is determined by the equation $\rho_a t_a \underline{a} = \sum_{j=1}^{m} \rho_j t_{aj} \underline{a}_j$, which defines the equivalent single source. The distribution of mass thickness of any evaporated film, when atoms stick where they strike, is therefore given by eq. 1, with values θ_a, φ_a determined by the distribution of sources. The replica may be called an *incidence-shaded* replica.

(b) Calculated Thickness When a Fraction of the Incident Atoms Diffuses Over the Surface

Figure 3 has shown that, in the case of silica, a fraction α of the impinging molecules stick where they first strike, the remainder diffusing. If the latter condense into a film of uniform thickness normal to the local surface, the shading equation becomes

$$t_e = t_a \cos \theta_a \left[\alpha(1 + \tan \theta_a \cos \varphi_a \tan \theta \cos \varphi) + (1 - \alpha) \frac{A_0}{A} \cdot \frac{1}{\cos \theta} \right] \tag{4}$$

where A is the total surface area and A_0 its projection on the jk plane (Fig. 1). Many other materials, and in particular silicon monoxide and germanium, condense likewise with values of α less than unity.

The assumption of uniform local thickness for the diffusing component is not quite correct. More strictly, A_0/A in eq. 4 should be evaluated over areas of the order of the square of the range ($\frac{1}{2}\mu$). Since the range is large compared to the resolution, and since A_0/A can only be estimated in any event, this refinement is of little value. It has been suggested[9] that diffusing silica has a higher probability of condensing in regions of change of gradient. This suggestion is difficult to sustain theoretically; further, observations upon thin shell replicas such as those of Fig. 3 have tended to indicate almost-uniform condensation.

(c) Replica Contrast as Determined by Relative Thickness vs. Colatitude Angle Curves

In any photographic presentation, two densities are detectably different

only if they differ by some small fraction on the density scale. Correspondingly, a finite difference in t_e is required. For 50 kv electrons, the minimum *perceptible* contrast difference is produced by a mass thickness difference of about 0.7 $\mu g/cm^2$. By plotting eq. (4) for particular choices of θ_a, φ_a and assumed values of α and A_0/A, the geometrical conditions required to pro-

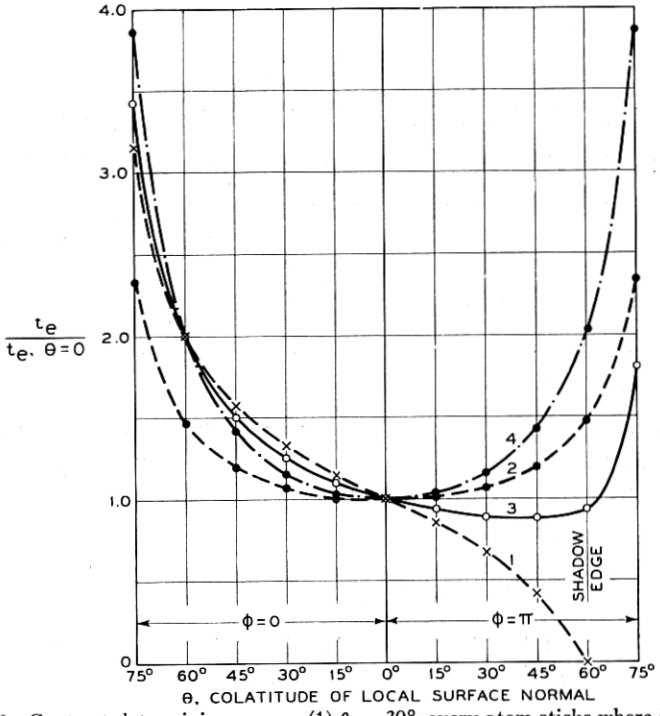

Fig. 16—Contrast-determining curves. (1) $\theta_a = 30°$, every atom sticks where it strikes. (2) $\theta_a = 0°$, half the atoms diffuse. (3) $\theta_a = 30°$, half the atoms diffuse. (4) $\theta_a = 0°$, all atoms diffuse over surface.

duce detectable differences in shading can be displayed. To make the curves more general, relative thickness rather than t_e is plotted in Fig. 16 for azimuth $\varphi_a = 0$. The four curves are, respectively, for

$$(1)\ \theta_a = 30°, \quad \alpha = 1, \qquad (2)\ \theta_a = 0°, \quad \alpha = \tfrac{1}{2},$$

$$(3)\ \theta_a = 30°, \quad \alpha = \tfrac{1}{2}, \qquad (4)\ \theta_a = 0°, \quad \alpha = 0.$$

A_0/A has been chosen as 0.833.

Let us assume that ρt_e when $\theta = 0$ is 7 $\mu g/cm^2$. Then a thickness difference of 0.1 on the ordinate scale is barely perceptible. For incidence shading,

curve (1) shows that two adjacent planes differing in colatitude angle by not less than 7° in the azimuth of incidence are detectable. For pure diffusion shading,* curve (4) shows that considerably larger differences in angle are required near $\theta = 0$; moreover, planes differing by large angles but symmetrical with respect to the electron beam yield the same t_e and hence, if adjacent, cannot be detected. This difference between diffusion and incidence shading is even more pronounced, because curve (4) is independent of azimuth, whereas for curve (1), $(1 - t_e/t_{e,\theta=0})$ is proportional to $\cos\varphi$. Although this introduces very low contrast in azimuths near $\varphi = 90°$, and also the possibility that two adjacent planes differing considerably in azimuth may yield the same density, incidence shading remains in general more favorable for portrayal of surface topography.

The intermediate curves (2) and (3) for $\alpha = \frac{1}{2}$ correspond to the case of condensation of silica at $\theta_a = 0°$ and 30° respectively. It is evident that, at normal incidence, appreciable contrast occurs only on the steeper slopes ($\theta > 45°$), and that *incidence at an angle is much to be preferred for general surface portrayal.*

APPENDIX II
RESOLUTION OF REPLICA FILMS

a) Incidence Shading

Figure 2 (a) shows, for the case of pure incidence shading, the replica film formed at the intersection of two surfacial planes with normals $\underline{n}_1$ and $\underline{n}_2$. The distance d over which the thickness changes from t_{e1} to t_{e2} is

$$d = t_a \sin\theta_a. \tag{5}$$

The figure is drawn for the case $\varphi_2 = 0$, $\varphi_1 = \pi$. More generally, if β is the azimuth of the line of intersection of the planes, it may be shown that

$$d = t_a \sin\theta_a \,|\sin\beta|. \tag{6}$$

The angle β is easily measured on a micrograph.
In vector notation,

$$d = t_a \left| \frac{(\underline{n}_1 \times \underline{n}_2) \times i}{|(\underline{n}_1 \times \underline{n}_2) \times i|} \cdot \underline{a} \right|$$

Or, in polar coordinates,

$$d = t_a \sin\theta_a \frac{|\tan\theta_1 \cos\varphi_1 - \tan\theta_2 \cos\varphi_2|}{(\tan^2\theta_1 + \tan^2\theta_2 - 2\tan\theta_1 \tan\theta_2 \cos(\varphi_2 - \varphi_1))^{\frac{1}{2}}}$$

* Aluminum or other oxide replica films formed by surface oxidation presumably correspond closely to the case $\alpha = 0$, which does not occur in evaporated films.

Using eq. (1)

$$d = \frac{| t_{e1} - t_{e2} |}{(\tan^2 \theta_1 + \tan^2 \theta_2 - 2 \tan \theta_1 \tan \theta_2 \cos (\varphi_2 - \varphi_1))^{\frac{1}{2}}} \tag{7}$$

For a given replica film the *intrinsic resolution* d varies simply as the sine of the azimuth of the line of intersection. For example, if $\theta_a = 30°$, d varies from $\frac{1}{2}t_a$ down to zero. But *observable* resolution is closely connected with contrast, as is indicated by eq. (7). One could not hope to *observe* good resolution if present, unless the thickness difference were at least two or three times the minimum perceptible thickness difference. In micrographs, because of the greater *contrast* characteristic of the azimuth $\beta \simeq 90°$, the resolution always appears best in the vicinity of the plane of incidence of the atom beam. The average thickness in the direction of the electron beam is $\bar{t}_e = t_a \cos \theta_a$ and hence:

$$d = \bar{t}_e \tan \theta_a \, | \sin \beta | \tag{8}$$

For $\theta_a = 30°$, $\sin \beta = 1$, $d = 0.577 \bar{t}_e$. If an attempt is made to improve resolution by decreasing θ_a, contrast is again reduced. It may be concluded that *the observable intrinsic resolution of an incidence-shaded replica film is not less than half the average thickness* $\bar{t}_e$.

b) Diffusion and Combined Shading

With pure diffusion shading,

$$d = t_n [\sin^2 \theta_1 + \sin^2 \theta_2 - 2 \sin \theta_1 \sin \theta_2 \cos (\varphi_2 - \varphi_1)]^{\frac{1}{2}} \tag{9}$$

Figure 2(b) illustrates this case for $\varphi_1 = \varphi_2 + \pi$. From eq. (4), for $\alpha = 0$, $| t_{e1} - t_{e2} | = t_n \left| \frac{1}{\cos \theta_1} - \frac{1}{\cos \theta_2} \right|$, since $t_n = t_a \cos \theta_a \frac{A_0}{A}$. Study of these two equations, for resolution and contrast respectively, shows that resolution is highly dependent on the relation of the local directions $\underline{n}_1$ and $\underline{n}_2$ to the incident electron beam: Values of d observable from a contrast standpoint frequently exceed $\bar{t}_e$, and are less than $\frac{1}{2}\bar{t}_e$ only when the two intersecting planes are fairly steep (θ_1 and $\theta_2 > 60°$) and are not too far apart in azimuth ($\varphi_2 \simeq \varphi_1$). *Hence the above conclusion also applies to pure diffusion shading, and consequently to combined shading such as that of a silica replica*, except possibly for special situations on steep slopes.

c) Shadow-edges

Shadow-edges are always due to the atoms that stick where they first strike, even though, as in the case of silica, part of the condensing material diffuses over the surface. Figure 17 illustrates the formation of a shadow-

edge by an obstacle of height h, whose profile is normal to the plane of the paper. From a point source, Fig. 17(a), the resolution is $d = l_a \sin \theta_a = \bar{l}_e \tan \theta_a$. More generally, if the profile makes an angle β with the plane of the paper, one obtains $d = \bar{l}_e \tan \theta_a \mid \sin \beta \mid$, identical with eq. (8). But now, because the contrast is large, the factor $\mid \sin \beta \mid$ is effective in im-

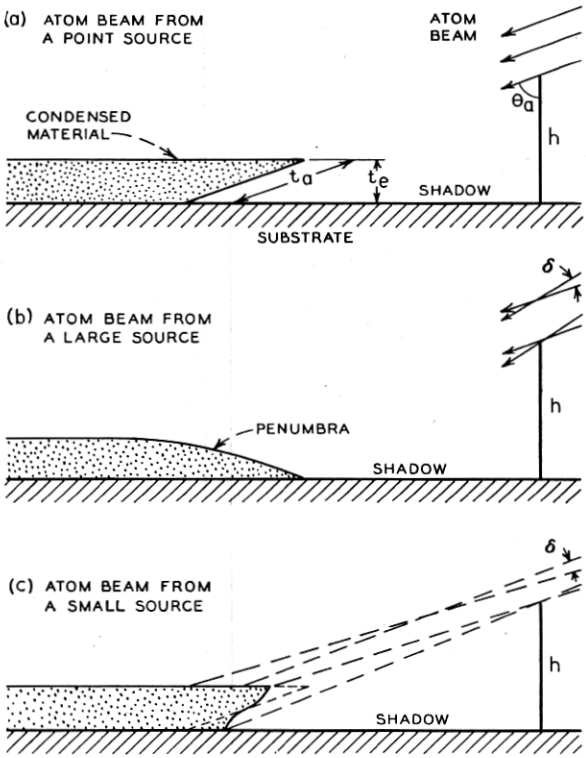

Fig. 17—Forms of shadow-edges when every atom sticks where it strikes.

proving the resolution. For example, one side of the shadow in the enlarged micrograph of Fig. 3 is very sharp.

Actual sources are of finite size, and in the cases illustrated in Fig. 17(b) and (c) the penumbra extends over a horizontal distance $p = h \sec^2 \theta_a \tan \delta$, where δ is the angle subtended by the source. If the source were of proper geometry and uniform intensity, one could set $p = d$ to obtain a vertical shadow-edge, whose intrinsic resolution would be zero. Actual sources are neither of proper geometry nor of uniform intensity, resulting in shadow-edges such as that of Fig. 17(c). If one takes into account a profile angle

β, and if h is so large that $p > d$, then somewhere along the side of the profile there should be a very sharp length of shadow-edge. In Fig. 3 the sharpest length of shadow-edge is neither at top nor at bottom of the side, but in an intermediate position.

In replicas other than those of particles which are dispersed on flat substrate surfaces, the topography of the surface in the shadow region is usually not planar. In general the form of the shadow-edge is a complicated function of $\underline{n}$, of the finite source, and of the profile casting the shadow. Its intrinsic resolution may vary from large values down to nearly zero. This last fact is important since it implies that *the intrinsic resolution of the sharpest portions of shadow-edges may often be assumed to be so small that the observed resolution is that of the microscope itself.* These remarks also apply to shadow profiles, for which the special conditions required for extreme sharpness probably occur more frequently than for shadow-edges.

d) Total Resolution

The intrinsic resolution of the film is only part of the total resolution, which includes also the resolution of the electron microscope. This is determined theoretically by the wave-length of the electrons (about 0.05Å) and the numerical aperture of the microscope (about 0.003) as modified by lens aberrations. The theoretical value of 10 Å is seldom attained in practice because of lens imperfections associated with use of the microscope. Practically, microscope resolution usually lies in the range 30–50 Å, for the RCA type EMU microscope with which the micrographs were taken. In the $\times$30,000 enlargements shown, 33 Å becomes 10^{-2} cm, just the limit of resolution of the eye. In general the resolution of the micrographs is not this good, in part because the intrinsic resolution is larger but also because it is necessary to find suitable fine-scale features to test the resolution.